Journal of ELECTRONIC MATERIALS, Vol. 39, No. 9, 2010
DOI: 10.1007/s11664-010-1331-0

Module Geometry and Contact Resistance of Thermoelectric Generators Analyzed by Multiphysics Simulation

D. EBLING,[1,2] K. BARTHOLOMÉ,[1] M. BARTEL,[1] and M. JÄGLE[1]

1.—Fraunhofer Institut IPM, Heidenhofstrasse 8, 79110 Freiburg, Germany. 2.—e-mail: dirk.ebling@ipm.fraunhofer.de

Thermoelectric device performance is determined by not only the properties of the thermoelectric material but also the geometrical design and thermal matching of the materials. Leg length and contact quality strongly influence thermoelectric generator efficiency. Experimental results for contact properties are compared with the latest performance measurements on modules manufactured from Bi_2Te_3 compounds. Module performance is related to the obtained contact resistance and thermoelectric material properties. The different influences are studied using thermoelectric multiphysics finite-element modeling of examples where, in addition to the thermoelectric field equations, further effects such as convection and radiation as well as the temperature dependency of the material properties are taken into account. Extensive thermoelectric device modeling is used to understand the experimental findings with respect to contact properties and geometry.

Key words: Thermoelectric generators, modeling, contact resistance, module geometry

INTRODUCTION

Good thermoelectric material properties are critical requirements for a thermoelectric module exhibiting high efficiency. Rowe and Min[1] describe the impact of the module's contact resistance on thermoelectric generator performance. Even with very good thermoelectric materials, device performance can be rather poor if the contact resistances of the module are too large.[2]

The figure of merit ZT of a thermoelectric generator is a measure of its performance and is closely related to the efficiency of a module.[3] It is strongly affected by the module resistance and is given by

$$ZT_{\text{module}} = \frac{\alpha^2 T}{K_{\text{module}} R_{\text{module}}},$$

where α denotes the Seebeck coefficient of the thermoelectric material, T is the average temperature of the module, and K_{module} and R_{module} are the heat conductance and total resistance of the module, respectively, given by

$$K_{\text{module}} = \frac{\lambda_n A_n}{l} + \frac{\lambda_p A_p}{l}$$

$$R_{\text{module}} = R_{\text{legs}} + R_{\text{c}} = \frac{\rho_n l}{A_n} + \frac{\rho_p l}{A_p} + R_{\text{c}}.$$

Here, A and l denote the cross-sectional area and length of the legs, respectively, and λ and ρ are the thermal conductivity and specific electric resistance, respectively. The resistance of the legs is given by R_{legs}, and the contact resistance is denoted by R_{c}. The subscripts n and p denote n- and p-type doping of the legs. The module ZT value can be rewritten as

$$ZT_{\text{module}} = ZT_{\text{mat}} \frac{1}{1 + R_{\text{c}}/R_{\text{legs}}}, \quad (1)$$

where ZT_{mat} denotes the ZT value of the material without contact resistance.

(Received July 10, 2009; accepted July 7, 2010; published online August 20, 2010)

For nonvanishing contact resistances of the module, its ZT value is always smaller than that achievable given the material's ZT value. However, the influence of the contact resistance R_c vanishes for increasing leg resistance R_{legs}. This suggests the possibility of minimizing the effect of contact resistances by increasing the length l of the thermoelectric legs, since the module's resistance R scales with l.

SIMULATIONS

These theoretical predictions were analyzed using finite-element analysis (FEA) simulations of the model shown in Fig. 1, following the approach of Jägle et al.[4,5] Figure 2 shows the impact of the contact resistance on the module ZT value for different lengths of the thermoelectric legs, showing that the decrease in ZT with contact resistance is reduced for longer thermoelectric legs. Figure 3 also supports these findings as a function of the device cold-side temperature T_K. The maximal module performance at $T_K \approx 360$ K results from the temperature-dependent material properties of the thermoelectric legs used in these simulations.[2] For these simulations, the contact resistance was assumed to be $R_c = 10$ mΩ. For the entire temperature range, the modules with 10 mm leg size performed clearly better than the modules with leg sizes of 6 mm and 3 mm.

MODULE FABRICATION

To verify the simulation results experimentally, modules with different leg sizes were fabricated. The manufacturing steps from the wafers produced by spark plasma sintering (SPS)[6,7] to thermoelectric modules with different leg sizes are illustrated in Fig. 4. In the first processing step, both sides of the

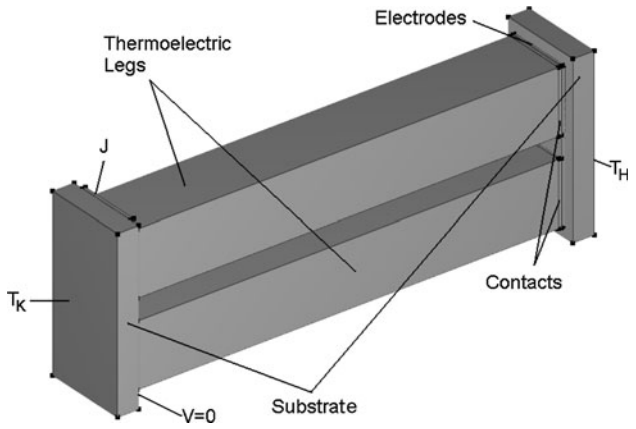

Fig. 1. Model of a pair of thermoelectric legs used for the FEA simulations. The simulated thermocouple consists of two legs with a base size of 1.5 mm × 1.5 mm. The legs are contacted with copper onto an alumina substrate. Contact resistances were simulated using an additional subdomain between the electrodes and the thermoelectric legs.

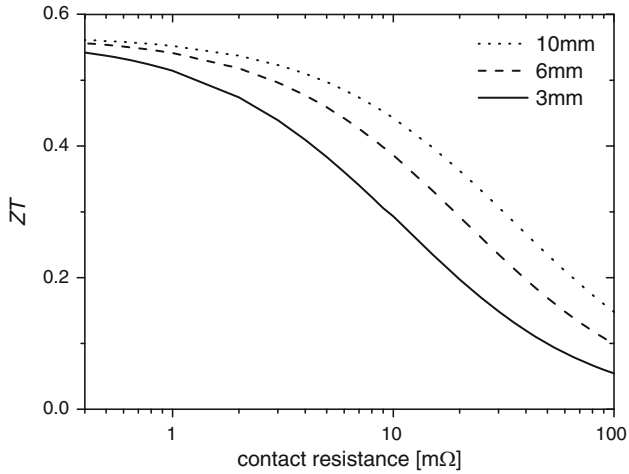

Fig. 2. Simulation results: impact of the contact resistance on the ZT value of the module for different leg sizes, calculated at room temperature. For vanishing contact resistance, the ZT values of the modules approach the maximum value of ~0.57 of the material applied. Modules with larger legs have a higher ZT value.

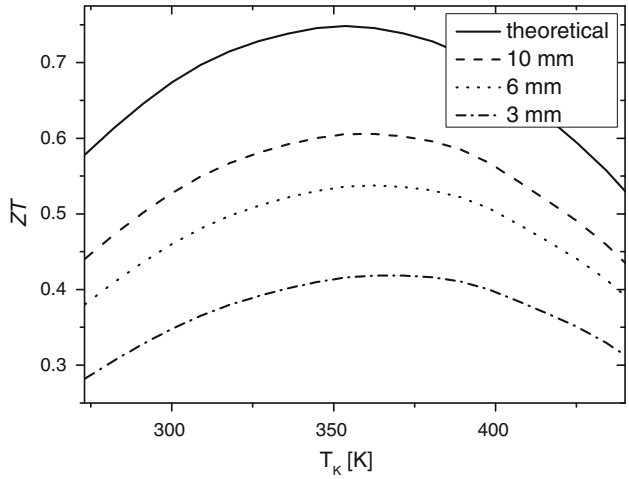

Fig. 3. Simulation results: module ZT values versus cold-side temperature T_K for different leg sizes. The simulations predict that modules with longer legs show better performance.

SPS wafers were polished to a thickness of 1.5 mm. Legs with a base area of 1.5 mm × 1.5 mm and length l of 3 mm, 6 mm, and 10 mm were cut from polished n- and p-doped SPS wafers using a wafer saw. After the determination of the thermoelectric properties of these legs, they were soldered to an Al_2O_3 substrate with contact pads by connecting the legs electrically in series and thermally in parallel, building modules with two and eight thermoelectric leg pairs, respectively. To minimize the contact resistance, different commercial solders were tested and compared, yielding very different contact resistances and hence ZT values of the modules (Table I). In Fig. 5, simulation results for the temperature-dependent ZT values are displayed for different solders according to Eq. 1. For each solder,

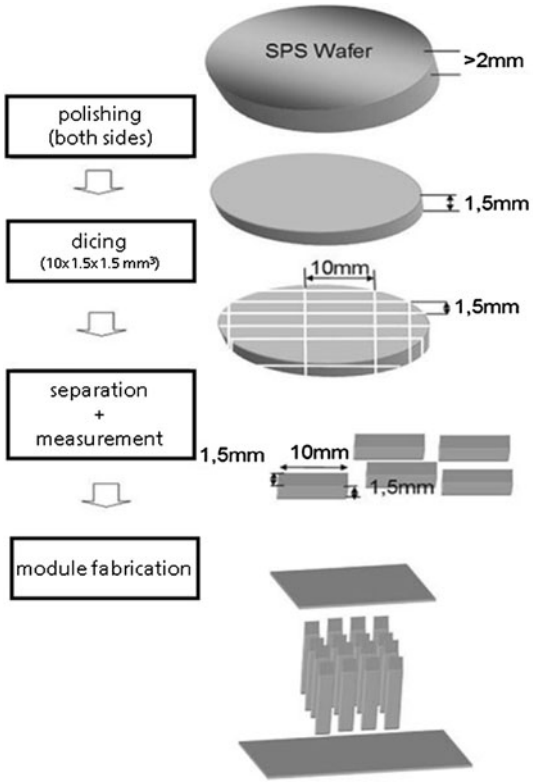

Fig. 4. Production of a thermoelectric module from SPS material.

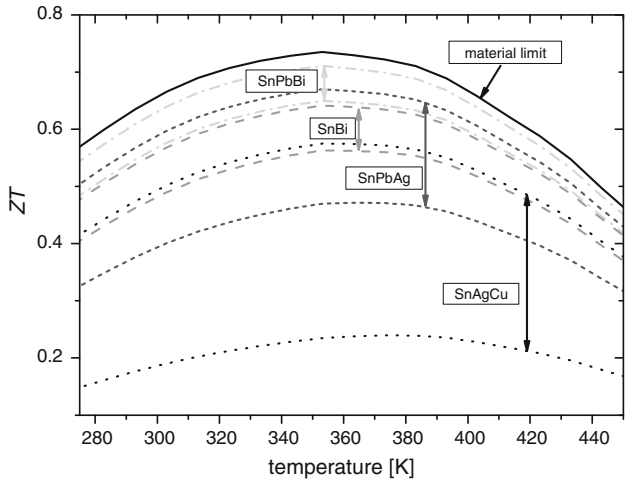

Fig. 5. Simulation results of the *ZT* value for different solders. The minimum and maximum values of contact resistance given in Table I were used to determine the range of *ZT* values as a function of temperature for each solder. The black curve shows the theoretical limit determined by the material properties.

Table I. Impact of different solders on contact resistance

Solder	ZT_{max}	Contact Resistance (mΩ)
SnPbBi	0.41	0.5–1.9
SnBi	0.31	1.4–8.1
SnPbAg	0.25	2.1–4.4
SnAgCu	0.23	4.0–30.6

The contact resistance can vary by up to two orders of magnitude depending on the solder.

a range of *ZT* values is given, corresponding to the range of the experimentally determined contact resistances. The *ZT* value for modules with SnPbBi solder is up to five times larger than the *ZT* value for modules fabricated with SnAgCu solder. The best solder material results in *ZT* values for modules approaching the theoretical limit determined by the material properties (black line in Fig. 5).

Experimentally, the *ZT* values, electric resistances, and maximum ΔT were measured for each module using a LTD Z-Meter model DX4065 (RMT Ltd.). This commercial device determines the thermoelectric parameters by applying the Harman method.[8] A short current pulse is applied to the module to produce a temperature gradient along the thermoelectric legs. The voltage drop along the module resulting from this temperature gradient is determined, enabling calculation of the desired thermoelectric parameters.[9] The experimental setup of the commercial equipment was modified to perform measurements not only at room temperature but also up to at least 300°C.

MEASURING THE CONTACT RESISTANCE

In a first approach, the contact resistance was calculated from the difference between the measured total resistance of the module and the sum of the resistances of each thermoelectric leg. Therefore, the electric conductivity of each single leg was determined in advance.

For validation, an alternative method to determine the contact resistance was applied by measuring the distribution of the resistance directly across the module. Therefore, the voltage drop generated by a pulsed current was measured using a contact tip at a certain position on the thermoelectric leg. By scanning the contact tip across the module, the resistance can be measured along the leg length, point by point. Figure 6 shows a series of these measurements for a module with large contact resistance assembled from two pairs of legs. The linear increase of resistance is caused by the electric conductivity of the thermoelectric material. The discontinuities result from the contact resistances of the solder. Thus, the actual contact resistance of each solder joint can be determined by measuring the difference of the resistance before and after the solder. The sum of the individual contact resistances then gives the total contact resistance of the module.

Figure 7 compares directly the measured total module resistance with the sum of individually

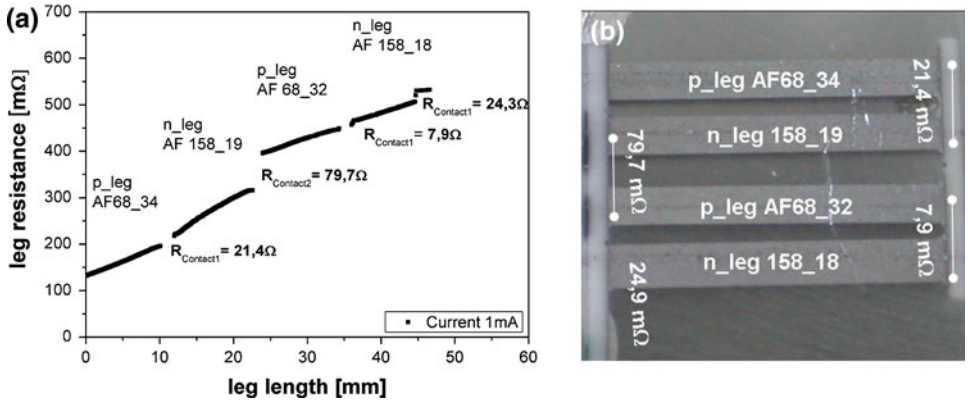

Fig. 6. Example results of measurement of the contact resistance of a module. The discontinuities represent the contact resistances, the linear slopes the resistance of the thermoelectric legs.

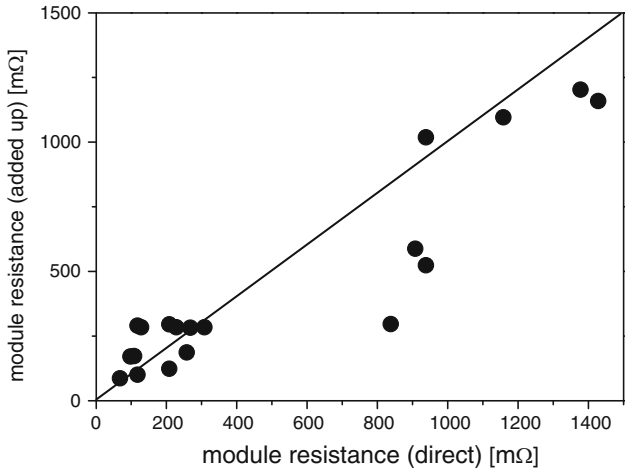

Fig. 7. Comparison of experimental module resistances: directly measured module resistances (*x*-axis) versus module resistances calculated by summing the individually measured resistances from its constituents (*y*-axis). Deviations from the bisecting line represent the uncertainty of the measuring method.

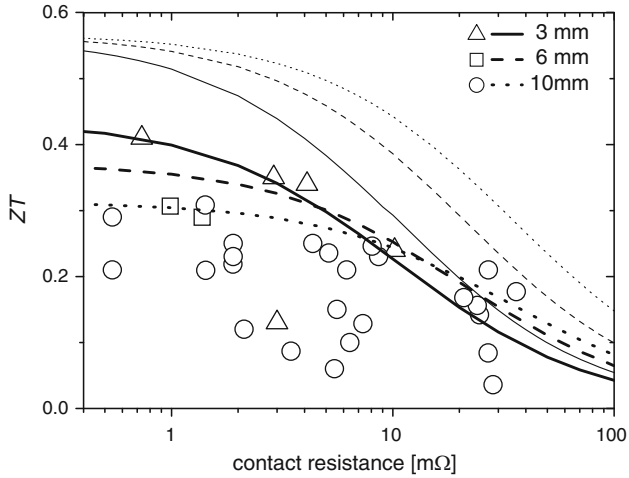

Fig. 8. Impact of contact resistance on module *ZT* value for different module lengths: comparison of experimental results (*triangles*, *squares*, and *circles*) with simulation results, with (*thicker lines*) and without (*thinner lines*) the inclusion of radiative and convective heat losses. Variation of line types refers to different length of the legs used in the simulation. The depiction of line types in the figure holds for thin and thick lines.

obtained point-by-point resistances of a module. Deviations from the bisecting line are caused by the uncertainties of the measuring methods.

EXPERIMENTAL RESULTS

For comparison with the theoretical predictions, several modules with leg lengths of 3 mm, 6 mm, and 10 mm were built according to the procedure described in Fig. 1. The *ZT* values and contact resistances were determined for each module using the methods described above. The results are depicted in Fig. 8. In agreement with Eq. 1 and the FEA simulation results, the *ZT* values of the modules increase as the contact resistance decreases. However, in contrast to the theoretical predictions (Fig. 2), modules built with legs of 3 mm length show better performance than modules with longer legs.

However, the theoretical prediction of Fig. 2 does not account for the impact of heat loss along the thermoelectric legs due to convection and radiation. The inclusion of these effects (thick lines, Fig. 8) yields good agreement of the theoretical predictions with the experimental data (details of the simulations are given in Bartholomé et al.[10]). The simulation takes into account heat losses based on the measurement of the emissivity of the thermoelectric material. For convection, an assumption was made by defining an average heat transfer coefficient, which is in agreement with the experimental results. However, in detail this can be only a rough estimate due to the unknown local temperatures of the transporting air and the type of convective flow. Inclusion of heat loss could also explain the inverse dependence of the performance on the length of the legs (Fig. 8). From the simulation it is shown that

the most evident influence is due to convection. Detailed experimental analysis is postponed to future investigations, which will be carried out in vacuum to suppress the convective part. Also the potential influence of radiation shields has to be tested for a better understanding. These uncertainties may also be responsible for the broad scatter of the measured *ZT* values with leg length. Detailed analysis is still difficult at this state without further experimental results.

CONCLUSIONS

In this work, the impact of contact resistance on module performance has been investigated. Following theoretical investigations and simulation results, a number of modules with different leg sizes were produced to analyze the influence of leg length and the negative effect of contact resistance on the *ZT* values of thermoelectric generators. Various solder materials were used to reduce the value of contact resistance. The prediction of better performance with smaller contact resistance could be verified for our manufactured modules. However, the prediction that module performance increases with leg length was not supported by the experiments. Further analysis showed that heat losses along the thermoelectric legs by convection and radiation are mainly responsible for this deviation.

REFERENCES

1. D.M. Rowe and G. Min, *IEE Proc. Sci. Meas. Technol.* 143, 351 (1996).
2. D. Ebling, M. Jaegle, M. Bartel, A. Jacquot, and H. Böttner, *J. Electron. Mater.* 38, 1456 (2009).
3. J. Yang and T. Caillat, *MRS Bull.* 31, 224 (2006).
4. M. Jaegle, M. Bartel, D. Ebling, A. Jacquot, and H. Böttner, *Proceedings of the 6th European Conference on Thermoelectrics*, Paris, France, 2–4 July 2008.
5. M. Jaegle, *Proceedings of the 5th European Conference on Thermoelectrics*, Odessa, Ukraine, 10–12 September, 2007.
6. H. Böttner, D. Ebling, A. Jacquot, J. König, L. Kirste, and J. Schmidt, *Phys. Stat. Sol. (RRL)* 1, 235 (2007).
7. D. Ebling, A. Jacquot, M. Jägle, H. Böttner, U. Kühn, and L. Kirste, *Phys. Stat. Sol. (RRL)* 1, 238 (2007).
8. T.C. Harman, *J. Appl. Phys.* 29, 1373 (1958).
9. A. Jacquot, M. Jägle, J. König, D.G. Ebling, and H. Böttner, *Proceedings of the 5th European Conference on Thermoelectrics*, Odessa, Ukraine, 10–12 September, 2007.
10. K. Bartholome, M. Bartel, M. Jägle, and D. Ebling, *J. Electron. Mater.*, 39(9), (2010).